ACES Asian Chemical Editorial Society

DOI: 10.1002/asia.202001311

CHEMISTRY AN ASIAN JOURNAL Full Paper

Large Nonlinear Optical Activity of a Near-infrared-absorbing Bithiophene-based Polymer with a Head-to-head Linkage

Can Ren,[a] Shuyu Xiao,[b, c] Junzi Li,[a] Lin Ma,[d] Rui Chen,*[e] Chuanxiang Ye,[f] Yang Gao,[b] Chenliang Su,*[a] and Tingchao He*[b, c]

Abstract: Although the production of near-infrared (NIR)-absorbing organic polymers with an excellent nonlinear optical (NLO) response is vital for various optoelectronic devices and photodynamic therapy, the molecular design and relevant photophysical investigation still remain challenging. In this work, large NLO activity is observed for an NIR-absorbing bithiophene-based polymer with a unique head-to-head linkage in the NIR region. The saturable absorption coefficient and modulation depth of the polymer are determined as $\sim -3.5\times10^{5}$ cm GW^{-1} and ~32.43%, respectively. Notably, the polymer exhibits an intrinsic nonlinear refraction index up to ~ -9.36 cm^2 GW^{-1}, which is six orders of magnitude larger than that of CS_2. The maximum molar-mass normalized two-photon absorption cross-section (σ_2/M) of this polymer can be up to ~14 GM at 1200 nm. Femtosecond transient absorption measurements reveal significant spectral overlap between the 2PA and excited state absorption in the 1000–1400 nm wavelength range and an efficient triplet quantum yield of ~36.7%. The results of this study imply that this NIR-absorbing polymer is promising for relevant applications.

Introduction

Nonlinear optical (NLO) materials have attracted considerable attention because of their potential applications in optoelectronics, such as laser Q-switching or mode-locking, optical limiters, and all-optical switches.[1] Various NLO materials have been reported, including two-dimensional materials,[2] semiconductor nanocrystals,[3] and organic molecules.[4] Although the rich electronic structure of these two-dimensional materials results in NLO responses over the ultraviolet terahertz to microwave regimes, a precise determination of the layer number remains difficult.[5] Although semiconductor nanocrystals with a large NLO response in the near-infrared (NIR) region can be designed, the application of these materials is hindered by poor environmental stability and long-term toxicity to biological tissues.[6] In contrast, organic molecules offer clear advantages, such as a low production cost, low toxicity, an adjustable molecular structure and a high exciton binding energy. Therefore, the development of organic molecules with excellent NLO responses is vital for practical applications.

The advantages of NLO behavior in the NIR region go beyond those associated with the visible region, especially for applications to deep-tissue bioimaging and photodynamic therapy and information communication.[7] Therefore, the development of NLO organic molecules with a NIR response is urgently required. Among these materials, thiophene derivatives have been shown to be a class of excellent optoelectronic materials with high photothermal stability.[8] Although excellent NLO activities for thiophene derivatives have been reported,[9] in-depth studies on optimized materials are still needed. Among various molecular design strategies, the design of organic molecular structures with large π-conjugated systems, good planar rigidity, and/or strong electron donors/acceptors has been proven to efficiently produce a large NLO response.[10]

Consequently, the Z-scan technique was used in this study to investigate the NLO response of a NIR-absorbing bithiophene-based polymer in detail. The high-performance donor constructed by unique head-to-head linkage (noncovalent sulfur-oxygen interaction) enables efficient intramolecular charge transfer (ICT) of the polymer, resulting in large NLO responses. The studies on the dynamic processes of the polymer reveal there are significant spectral overlap between 2PA and excited state absorption (ESA) and efficient intersystem crossing (ISC).

[a] C. Ren, J. Li, Prof. C. Su
SZU-NUS Collaborative Center, International Collaborative Laboratory of 2D Materials for Optoelectronic Science & Technology of Ministry of Education, Engineering Technology Research Center for 2D Materials Information Functional Devices and Systems of Guangdong Province, Institute of Microscale Optoelectronics, Shenzhen University, 518060 Shenzhen (P. R. China)
E-mail: chmsuc@szu.edu.cn

[b] S. Xiao, Prof. Y. Gao, Prof. T. He
Key Laboratory of Optoelectronic Devices and Systems of Ministry of Education and Guangdong Province, College of Physics and Optoelectronic Engineering, Shenzhen University, 518060 Shenzhen (P. R. China)
E-mail: tche@szu.edu.cn

[c] S. Xiao, Prof. T. He
Key Laboratory for Organic Electronics and Information Displays, Institute of Advanced Materials (IAM), Nanjing University of Posts & Telecommunications, 9 Wenyuan Road, 210023 Nanjing (P. R. China)

[d] Prof. L. Ma
School of Physics and Optoelectronic Engineering, Guangdong University of Technology, 510006 Guangzhou (P. R. China)

[e] Prof. R. Chen
Department of Electrical and Electronic Engineering, Southern University of Science and Technology, 518055 Shenzhen (P. R. China)
E-mail: chenr@sustech.edu.cn

[f] Dr. C. Ye
Shenzhen Institute of Information Technology,
518172 Shenzhen (P. R. China)

Results and Discussion

The polymer has a D-A type structure with a unique head-to-head linkage (Figure. 1a), in which two thienyl groups (3-alkoxy-3′-alkyl-2,2′-bithiophene) are connected through intramolecular noncovalent sulfur-oxygen interaction. In the polymer, the bithiophene unit serves as the electron donor and the benzothiadiazole unit serves as the electron acceptor. The alkyl groups on two side chains are employed to improve the solubility of the polymer. As shown in Figure 1b, the polymer exhibits an uncharacteristic absorption curve, with an absorption band peak at 720 nm (S_0–S_1 transition) and a shoulder at 412 nm (S_0–S_n transition). In addition, the polymer exhibits a much weak photoluminescence (PL) emission at 795 nm, with a low absolute quantum yield of 0.074% because of the forbidden n–π* transition.[11] The HOMO and LUMO energies were calculated to be −4.65 and −2.25 eV, respectively, with a strong oscillation strength of 0.5448 and a transition probability of 70% (Figure 1c). These parameters indicate that the effective ICT was mainly caused by the HOMO to LUMO transition.

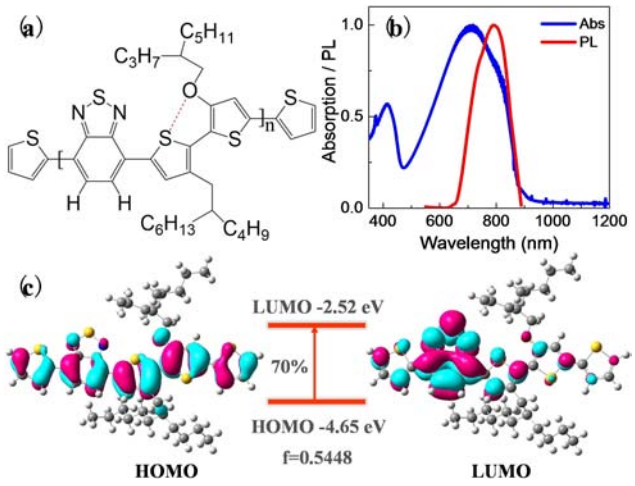

Figure 1. a) Polymer molecular structure (the intramolecular noncovalent sulfur–oxygen interaction is indicated by red dashed line). b) normalized absorption and PL spectra of polymer in THF solution. and c) molecular orbital transitions corresponding to S_0–S_1 transition and energy level distribution.

The n_2 value of the polymer was then obtained by dividing the closed-aperture Z-scan data by the open-aperture values at 800 nm, as shown in Figure 2a. It can be seen that the CS_2 and THF solvent exhibit positive nonlinear refraction and self-focusing effect. In contrast, negative nonlinear refraction and self-defocusing effect were observed for the polymer solution. The procedure described in Ref. [12] was used to calculate nonlinear refractive index (n_2) for the polymer solution and THF as $\sim -6.2\times10^{-6}$ cm^2 GW^{-1} and $\sim 1.57\times10^{-6}$ cm^2 GW^{-1}, respectively. The following equation (1) was used to calculate the polymer intrinsic n_2 as ~ -9.36 cm^2 GW^{-1}.[13]

$$n_2\ solution \quad 1 - f\ n_2\ solvent \quad f n_2\ solute \tag{1}$$

where f is the solute mole fraction. Surprisingly, this value is 6 orders of magnitude larger than that of CS_2 and several orders of magnitude larger than those of many NIR-absorbing materials reported thus far, including $MAPbI_3$ ($\sim 9.5\times10^{-5}$ cm^2 GW^{-1} at 1000 nm),[14] $CsPb(Cl_{0.53}Br_{0.47})_3$ ($\sim -1.4\times10^{-4}$ cm^2 GW^{-1} at 620 nm),[15] $MoTe_2$ film (~ -1.24 cm^2 GW^{-1} at 800 nm),[16] WS_2 film (~ -8.1 cm^2 GW^{-1} at 800 nm)[17] and some organic molecules, such as Zn-terpyridine polymer ($\sim 1.1\times10^{-4}$ cm^2 GW^{-1} at 765 nm).[18] The large n_2 of our polymer might be attributed to the unique head-to-head linkage (noncovalent interactions between pairs of sulfur and oxygen atoms). On one hand, the non-covalent bonding between sulfur-oxygen atoms can enhance the molecular planar rigidity of the donor.[19] On the other hand, the polymer possesses strong electron-withdrawing and -donating ability, thereby improving the ICT within the molecule. The abovementioned two factors can efficiently amplify the NLO activity of the polymer. In addition, the intrinsic n_2 values of our polymer is compared with other NLO materials in Table 1.

The open-aperture Z-scan measurement also showed strong saturable absorption of the polymer (Figure 2b). The saturable absorption coefficient of the polymer solution was calculated as β (solution) ~ -0.29 cm GW^{-1}. The corresponding intrinsic saturable absorption coefficient of the polymer was calculated as β (intrinsic) $\sim -3.5\times10^5$ cm GW^{-1}. The excitation-light-intensity-dependent transmittance was then measured to determine the saturation intensity and modulation depth of the polymer solution (Figure 2c). The experimental data could be fitted by the following equation (2).

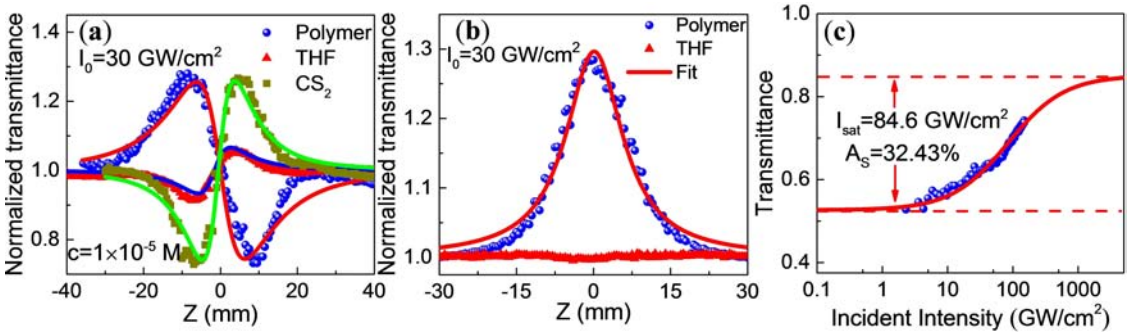

Figure 2. Z-scan curves at 800 nm. a) close-aperture results divided by open-aperture results and (b) open-aperture result. c) NLO transmittance curve recorded at 800 nm. Experimental data was fit using Eq. 2 to yield a saturable intensity of ~84.6 GW cm^{-2} and a modulation depth of ~32.43%.

Table 1. Comparison of NLO parameters for polymer used in this study and various materials reported in the literature.

Materials	Laser	β [cm GW^{-1}]	n_2 [cm^2 GW^{-1}]	Ref.
$MAPbM_3$ single crystal	1000 nm, 70 fs	5.2	9.5×10^{-5}	14
$CsPb(Cl_{0.53}M_{0.47})_3$ nanocrystals	620 nm, 100 fs	3.22×10^{-3}	-1.4×10^{-4}	15
$MoTe_2$ film	800 nm, 100 fs	-7.4×10^{5}	−1.24	16
Monolayer WS_2 film	800 nm, 100 fs	-3.7×10^{5}	−8.1	17
Zn-terpyridine polymer	765 nm, 100 fs	N.A.[a]	1.1×10^{-4}	18
GePOvinylidene fluoride film	800 nm, 100 fs	−0.474	5.4×10^{-6}	20
Mthiophene-based polymer	800 nm, 100 fs	-3.5×10^{5}	−9.36	This work

[a] Not available.

$$T \quad 1 - A_s / \ 1 \quad I/I_{sat} \qquad (2)$$

where A_s represents the modulation depth, I_0 is the incident light intensity, and I_{sat} is the saturation light intensity. The resulting A_s and I_{sat} of the polymer solution were ~32.43% and ~84.6 GWcm^{-2}, respectively. The A_s of polymer solution was even larger compared with many saturable absorption materials, such as black phosphorus and MoS_2,[21] and M_2Te_3–$FeTe_2$ nanoplates.[22] Therefore, our polymer may be a promising saturable absorber for laser Q-switching or mode-locking. Table 2 is a comparison of the properties of various NLO materials.

The large NLO activities in the resonant absorption band motivated the expectation of a strong 2PA for wavelengths above 1000 nm. The open-aperture Z-scan technique was used to determine the 2PA coefficient of the polymer. Figure 3a is a typical open-aperture Z-scan curve under 1050 nm excitation. The reduced transmittance of the incident light intensity at the focus point evidenced 2PA. Curve fitting yielded a 2PA coefficient of the polymer solution β ~0.05 cm GW^{-1}. This value is extremely large, considering the very low polymer solution concentration (~1×10^{-5} M).

A large 2PA saturable intensity (I_{sat}) for NLO materials is required for 2PA-based applications. Therefore, the incident-light-intensity-dependent transmittance was measured to determine 2PA I_{sat} of the polymer at 1050 nm (Figure 3b). As the incident light intensity increased, the transmittance first rapidly decreased before approaching a constant, which resulted from

Table 2. Comparison of saturable absorption coefficient (β), saturation intensity (I_{sat}) and modulation depths (A_S) for polymer used in this study and various NLO materials reported in the literature.

Materials	β [cm GW^{-1}]	I_{sat} [GWcm^{-2}]	A_S [%]	Ref.
Menzotriazole-based copolymer dots	-6.6×10^{5} (100 fs, 1040 nm)	0.028	13	9c
GePOvinylidene fluoride film	-4.74×10^{-1} (100 fs, 800 nm)	76.48	20.48	20
Graphene dispersion	-8.28×10^{-3} (100 fs, 800 nm)	764	N.A.	21a
Mack phosphorus dispersions	-1.38×10^{-2} (100 fs, 800 nm)	459	N.A.	21a
MoS_2 dispersions	N.A. (100 fs, 800 nm)	279.6	34	21b
M_2Te_3–$FeTe_2$ nanoplates	-7.53×10^{-4} (100 fs, 800 nm)	314	13	22
Mthiophene-based polymer	-3.5×10^{5} (100 fs, 800 nm)	84.6	32.43	This work

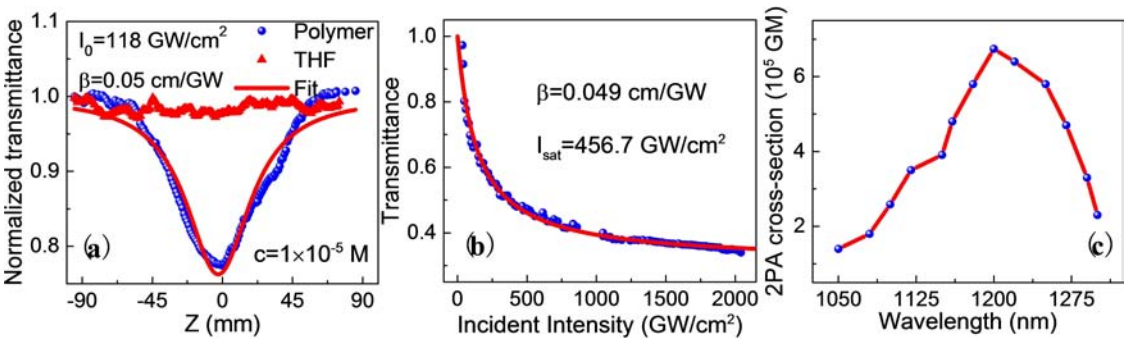

Figure 3. a) Open-aperture Z-scan curve at 1050 nmNb) excitation intensity dependent nonlinear transmittance at 1050 nmNand (c) 2PA cross-sections in 1050–1300 nm wavelength range.

the two-photon saturation effect. This process can be described using the following hyperbolic 2PA saturation model (equation 3)L[23]

$$\beta I \quad \beta / 1 \quad I/I_{sat} \tag{3}$$

The theoretical fit given by Eq. (3) was used to determine the 2PA coefficient (β) and I_{sat} value of the polymer as ~0.049 cm GW^{-1} and ~457.6 GW cm^{-2}, respectively. The 2PA coefficient was consistent with the Z-scan measurement. The large I_{sat} indicates that the polymer can be exploited in 2PA-based optoelectronic device applications. The 2PA cross-sections (σ) of the polymer were then determined under different excitation wavelengths (Figure 3c), where the maximum σ reached ~6.74×10^5 GM at 1200 nm, and the value is 1 to 4 orders of magnitude larger compared with other NIR-absorbing organic molecules[24] (Table 3). The 2PA performance is also reflected in so-called molar-mass normalized 2PA cross-sections (σ_2/M), which are the most widely used merit factors to assess the relative strength of 2PA processes.[25] The σ_2/M value of the polymer was calculated as ~14 GM that is much larger than many reported polymers.[26] In addition, the 2PA cross-section per repeat unit for the polymer is calculated as ~8.7×10^3 GM, which is among the largest values in previous reported NIR-absorbing materials.[27]

The excited-state lifetime of NLO materials is an important parameter for ultrafast optics applications. Therefore, under the excitation at 800 nm, the fs-TA spectra of the polymer were measured over the NIR range (1000–1400 nm), as shown in Figure 4a. A positive ESA band at 1000–1400 nm was clearly observed. The ESA can be characterized by a biexponential decay with lifetime values of ~4.2 and ~270 ps at 1200 nm, respectively. The fast process could be ascribed to the transfer process from the levels of the excited state to the ICT state, while the long process is attributed to the evolution of the ICT state.[28] The corresponding averaged lifetime was calculated as ~268 ps. Another important result was the significant overlap between the 2PA and ESA spectra of the polymer. When the pulse duration of excitation light is on the same order of magnitude as the lifetime of the molecular excited state (or even longer), a 2PA-induced ESA mechanism can be expected to produce efficient optical limiting of nanosecond pulses in the telecommunication wavelength range for our polymer.[29] The corresponding physical mechanism is shown in the inset of Figure 4b.

We further studied the ultrafast dynamics of the polymer in visible wavelength range (350–750 nm), under the excitation at 800 nm. It was found that there are two positive bands peaking at 475 and 719 nm (Figure 4a). Remarkably, accompanied by the decay of the band at 475 nm, another positive band peak at 719 nm gradually appears. Positive absorption centred at 475 nm corresponds to singlet–singlet transitions, whereas the positive absorption band at 719 nm is ascribed to the triplet-triplet transition. For more underlying information, the decay curves at the wavelengths of the singlet and triplet states were extracted and are presented in Figure 4c. The corresponding global fitting on the 475 and 719 nm traces resulted in one decay component of 3.8 ps and one rise component of 10.3 ps. Accordingly, the efficiency of ISC (Φ_{ISC}) was estimated to be $\Phi_{ISC}=(1/\tau_{rise})/(1/\tau_{decay})=36.7\%$. Such efficient ISC process may be ascribed to the relatively distorted molecular structure that was induced by the bithiophene and benzothiadiazole units.[30]

In order to explore the potential application of the polymer in photodynamic therapy, its relative singlet oxygen generation capacity in THF was further evaluated by using a chemical probe method. 1,3-diphenylisobenzofuran (I PMF) was chosen as a trap for singlet oxygen.[31] As a comparison, the control experiment was done in the presence of indocyanine green (ICG) under the same experimental condition.[32] As shown in

Table 3. Comparison of 2PA cross-sections for polymer used in this study and other NIR-absorbing molecules reported in the literature

Materials	σ [GM]	Refs
Thiadiazolo quinoxaline	168 (920 nm, 100 fs)	24a
MOI IPY	4×10^3 (1240 nm, 100 fs)	24b
Fused-ring quadrupolar polymer	2.7×10^4 (1346 nm, 100 fs)	24c
Benzothiadiazole tetraphenylethene dots	7.63×10^4 (1200 nm, 100 fs)	24d
Bithiophene-based polymer	6.7×10^5 (1200 nm, 100 fs)	This work

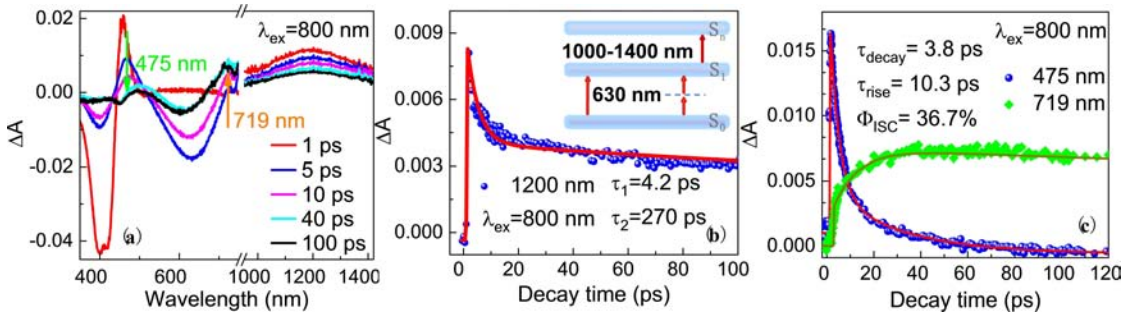

Figure 4. (a) fs-TA spectra of the polymer at different probe delay times following 800 nm laser excitation. (b) The kinetic profiles at 630 and 1200 nm. Inset is a schematic of 2PA-induced ESA mechanism for nanosecond pulses in 1000–1400 nm wavelength range. (c) The kinetic profiles at 475 and 719 nm.

Figure 5a and b, with the increase of irradiation time, the reaction of polymer in THF with singlet oxygen causes a significant decrease of the I PMF absorbance at 412 nm, while the decrease rate in presence of ICG is negligible. From the quantitative comparison of the I PMF photo-oxidation rate in presence of polymer and ICG (Figure 5c), it was revealed that the polymer possesses more efficient singlet oxygen generation capability and great promise in photodynamic therapy.

- onclusion

The Z-scan technique was used to investigate the NLO response of a NIR-absorbing bithiophene-based polymer with a head-to-head linkage. The electron-donating substituent constructed by a unique head-to-head linkage structure results in a large NLO over NIR wavelength range that is much stronger than those of many NLO materials, including organic molecules, inorganic semiconductor nanocrystals and two-dimensional materials. This result demonstrates the potential application of this polymer in ultrafast all-optical switching and laser Q-switching or mode-locking. The large overlap between the 2PA and ESA spectra may make the polymer an efficient broadband optical limiter for nanosecond pulses in the telecommunication wavelength range. In addition, the efficient ISC process and singlet oxygen generation in the polymer implies that it can be used as a photodynamic therapy agent.

. / perimental 0ection

1 aterials

The detailed synthesis procedure of the NIR-absorbing bithiophene-based polymer with a head-to-head linkage has been previously reported.[19]

Linear optical characteri2ation

An ultraviolet-visible-NIR spectrophotometer (Lambda 950) was used to measure the KV-visible absorption spectrum of the polymer. The polymer emission spectrum and quantum efficiency were determined using a FluoroSENS fluorescence spectrometer, which is equipped with a 150-W xenon lamp and an integrating sphere accessory. I uring the measurements, the polymer was dissolved into the THF solvent, and the resultant solution with a concentration of $\sim 1.0\times10^{-6}$ M was filled into a 1-cm cuvette.

NLO characteri2ation

Open- and closed-aperture Z-scan measurements were used to determine the nonlinear absorption coefficient (β) and nonlinear refraction index (n_2) of the polymer, respectively.[12] The light source was produced using a TiL sapphire laser oscillator, a regenerative amplifier system (Spectra-physics Spitfire Ace), and an optical parametric amplifier (OPA) combination system emitting at a center wavelength of 800 nm (1 kHz, 100 fs). The fs pulses in the 1050–1300 nm wavelength range were produced by TOPAS. The ultrashort pulse width (100 fs) and low repetition frequency (1 kHz) of the excitation light ensured that the thermal effect (in the ns range) on the measured NLO parameters was negligible.[33] The Z-scan setup was calibrated using CS_2 before performing the measurements, and the obtained n_2 value ($\sim 4.5\times10^{-6}$ cm^2 GW^{-1}) was consistent with that reported in the literature,[34] validating the Z-scan measurements. For all the NLO characterizations, the polymer solution concentration is 1×10^{-5} M filled into a 1-mm cuvette.

1 easurement of fs-A spectra

I uring the measurements, 800 nm pump pulses were generated from an OPA system combined with TOPAS, whereas probe pulses in the 1000–1400 nm range were generated by irradiating 800 nm fs pulses onto a YAG crystal. The polymer solution with a concentration of $\sim 1.0\times10^{-5}$ M was filled into a 1 mm-thick quartz liquid cell. The measurements were carried out at environmental condition.

Detection of 0inglet O/ygen 3eneration

Singlet oxygen generation was confirmed by using I PMF in THF as an indicator and ICG was used as the reference photosensitizer. I uring the measurement, an 808 nm continuous laser ($\sim$1 W cm^{-1}) was used as the excitation source.

heoretical calculation

I ensity functional theory and time-dependent density functional theory were used in conjunction with the Gaussian 09 software package to calculate the electronic structure parameters, including the oscillator strength, the orbital excitation energy, the orbital transition probability, and the highest and lowest occupied molecular orbitals (HOMO and LK MO, respectively).

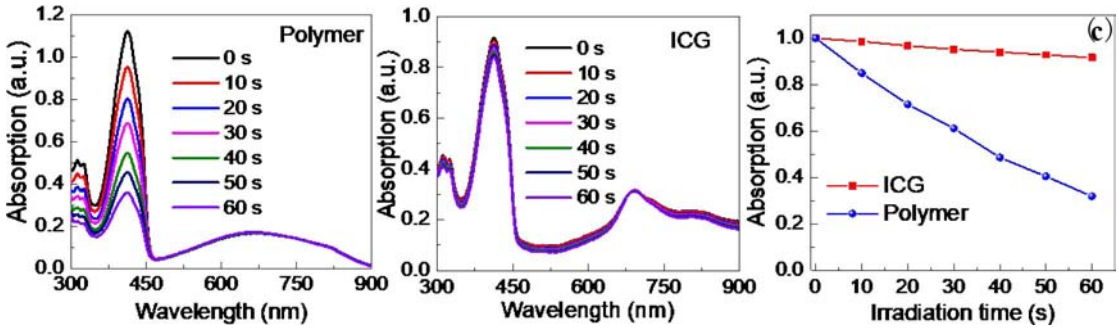

Figure 4. The absorption spectra of I PMF in THF as a function of irradiation time in the presence of polymer (a) and ICG (b). (c) The absorbance of I PMF at 412 nm as a function of irradiation time in the presence of polymer and ICG.

Acknowledgements

We would like to thank Prof. Xugang Guo from the Southern University of Science and Technology for providing the polymer sample for this study. This work was financially supported by the Open Research Fund of the Key Laboratory for Organic Electronics and Information Displays, the National Natural Science Foundation of China (1190A2A0, 1187A125), the Natural Science Foundation of Guangdong Province (2018A030310637, 2018A030310635) and the Science and Technology Planning Project of Shenzhen Municipality (JCYJ201708181A29210AA).

Conflict of Interest

The authors declare no conflict of interest.

Keywords: near-infrared-absorbing bithiophene-based polymer · saturable absorption · nonlinear refraction · two-photon absorption

[1] a) J. M. Hales, J. Matichak, S. Marlow, S. Ohira, P. Yesudas, J. L. Mredas, J. W. Perry, S. R. Marder, *Science* **2010**, *327*, 1485–1488Nb) G. S. He, L.-S. Tan, Q. Zheng, P. N. Prasad, *Chem. Rev.* **2007**, *108*, 1245–1330Nc) P. Han, I. Wang, H. Gao, J. Zhang, Y. Xing, Z. Yang, H. Cao, W. He, *Dyes Pigm.* **2017**, *1A9*, 8–15.
[2] a) X. Liu, Q. Guo, J. Qiu, *Adv. Mater.* **2018**, *29*, 1605886Nb) Y. Wang, M. Qiu, M. Won, E. Jung, T. Fan, N. Xie, S.-G. Chi, H. Zhang, J. S. Pim, *Coord. Chem. Rev.* **2019**, *A00*, 213041.
[3] a) J. Yu, Y. Rong, C. T. Puo, X. H. Zhou, I. T. Chiu, *Anal. Chem.* **2018**, *89*, 42–56Nb) J. Wang, Y. Mi, X. Gao, J. Li, J. Li, S. Lan, C. Fang, H. Shen, X. Wen, R. Chen, X. Liu, T. He, I. Li, *Adv. Opt. Mater.* **2019**, *7*Nc) G. Xing, M Wu, X. Wu, M. Li, M Iu, Q. Wei, J. Guo, E. P. L. Yeow, T. C. Sum, W. Huang, *Nat. Commun.* **2018**, *8*, 14558Nd) J. Guo, T. Liu, M. Li, C. Liang, P. Wang, G. Hong, Y. Tang, G. Long, S.-F. Yu, T.-W. Lee, W. Huang, G. Xing, *Nat. Commun.* **2020**, *11*, 3361.
[4] a) T. He, Y. Wang, X. Tian, Y. Gao, X. Zhao, A. C. Grimsdale, X. Lin, H. Sun, *Appl. Phys. Lett.* **201:** , *108*Nb) W. Hu, X. Miao, H. Tao, A. Maev, C. Ren, Q. Fan, T. He, W. Huang, P. N. Prasad, *ACS Nano* **2019**, *13*, 12006–12014Nc) X. Hou, J. Sun, Z. Liu, C. Yan, W. Song, H.-L. Zhang, S. Zhou, X. Shao, *Chem. Commun. (Camb.)* **2017**, *5A*, 10981–10984.
[5] S. Yu, X. Wu, Y. Wang, X. Guo, L. Tong, *Adv. Mater.* **2018**, *29*, 1606128.
[6] Y. Wang, Y. Wang, P. Chen, P. Qi, T. Xue, H. Zhang, J. He, S. Xiao, *ACS Nano* **2020**.
[7] a) G. Hong, A. L. Antaris, H. Iai, *Nat. Biomed. Eng.* **2018**, *1*Nb) J. Qi, C. Sun, I. Li, H. Zhang, W. Yu, A. Zebibula, J. W. Y. Lam, W. Xi, L. Zhu, F. Cai, P. Wei, C. Zhu, R. T. P. Pwok, L. L. Streich, R. Prevedel, J. Qian, M Z. Tang, *ACS Nano* **2017**, *12*, 7936–7945.
[8] N. M Teran, G. S. He, A. Maev, Y. Shi, M. T. Swihart, P. N. Prasad, T. J. Marks, J. R. Reynolds, *J. Am. Chem. Soc.* **201:** , *138*, 6975–6984.
[9] a) W. Shao, Q. Wei, S. Wang, F. Li, J. Wu, J. Ren, F. Cao, H. Liao, J. Gao, M. Zhou, I. Ling, *Mater. Horiz.* **2020**, *7*, 1379–1386N b) S. Anandan, S. Manoharan, N. P. S. Narendran, T. C. S. Girisun, A. M. Asiri, *Opt. Mater.* **2017**, *85*, 18–25Nc) H. Chen, F. Wang, M. Liu, M. Qian, X. Men, C. Yao, L. Xi, W. Qin, G. Qin, C. Wu, *Laser Photonics Rev.* **2019**, *13*, 1800326Nd) Z. Liu, J. Sun, C. Yan, Z. Xie, G. Zhang, X. Shao, I. Zhang, S. Zhou, *J. Mater. Chem. C.* **2020**, *8*, 12993–13000.
[10] a) S. Sasaki, G. P. C. I rummen, G.-i. Ponishi, *J. Mater. Chem. C.* **201:** , *A*, 2731–2743Nb) J. Jia, X. Wu, Y. Fang, J. Yang, X. Guo, Q. Xu, Y. Han, Y. Song, *J. Phys. Chem. C.* **2017**, *122*, 16234–16241Nc) S. Ellinger, P. R. Graham, P. Shi, R. T. Farley, T. T. Steckler, R. N. Mrookins, P. Taranekar, J. Mei, L. A. Padilha, T. R. Ensley, H. Hu, S. Webster, I. J. Hagan, E. W. Van Stryland, P. S. Schanze, J. R. Reynolds, *Chem. Mater.* **2011**, *23*, 3805–3817Nd) J. E. Ehrlich, X. L. Wu, I. Y. S. Lee, Z. Y. Hu, H. RQckel, S. R. Marder, J. W. Perry, *Opt. Lett.* **1998**, *22*, 1843–1845.
[11] W. Huang, M X. Mi, Z. Q. Gao, *Org. Electron.*, Science Press, Mei Jing, **2011**.
[12] M. Sheik-Mahae, A. A. Said, T. Wei, I. J. Hagan, E. W. V. Stryland, *IEEE J. Cuantum Electron.* **1990**, *26*, 760–769.
[13] G. S. He, J. Zhu, A. Maev, M. SamoR, I. L. Frattarelli, N. Watanabe, A. Facchetti, H. Sgren, T. J. Marks, P. N. Prasad, *J. Am. Chem. Soc.* **2011**, *133*, 6675–6680.
[14] C. Priso, M. Stein, T. Haeger, N. Pourdavoud, M. Gerhard, A. Rahimi-Iman, T. Riedl, M. Poch, *Opt. Lett.* **2020**, *A5*, 2431–2434.
[15] J. Li, C. Ren, X. Qiu, X. Lin, R. Chen, C. Yin, T. He, *Photonics Res.* **2017**, *6*.
[16] J. Wang, H. Chen, Z. Jiang, J. Yin, J. Wang, M. Zhang, T. He, J. Li, P. Yan, S. Ruan, *Opt. Lett.* **2017**, *A3*, 1998–2001.
[17] X. Zheng, Y. Zhang, R. Chen, X. Cheng, Z. Xu, T. Jiang, *Opt. EDpress* **2014**, *23*, 15616–15623.
[18] T. He, I. Rajwar, L. Ma, Y. Wang, Z. Mang Lim, A. C. Grimsdale, H. Sun, *Appl. Phys. Lett.* **2012**, *101*.
[19] S. Shi, Q. Liao, Y. Tang, H. Guo, X. Zhou, Y. Wang, T. Yang, Y. Liang, X. Cheng, F. Liu, X. Guo, *Adv. Mater.* **201:** , *28*, 9969–9977.
[20] J. Guo, I. Huang, Y. Zhang, H. Yao, Y. Wang, F. Zhang, R. Wang, Y. Ge, Y. Song, Z. Guo, F. Yang, J. Liu, C. Xing, T. Zhai, I. Fan, H. Zhang, *Laser Photonics Rev.* **2019**, *13*, 1900123.
[21] a) P. Wang, M M. SzydTowska, G. Wang, X. Zhang, J. J. Wang, J. J. Magan, L. Zhang, J. N. Coleman, J. Wang, W. J. Mau, *ACS Nano* **201:** , *10*, 6923–6932Nb) H. Zhang, S. M Lu, J. Zheng, J. I u, S. C. Wen, I. Y. Tang, P. P. Loh, *Opt. EDpress* **201**, *22*, 7249–7260.
[22] L. Zhang, J. Liu, J. Li, Z. Wang, Y. Wang, Y. Ge, W. I ong, N. Xu, T. He, H. Zhang, W. Zhang, *Laser Photonics Rev.* **2020**, *1A*, 1900409.
[23] J. F. Lami, P. Gilliot, C. Hirlimann, *Phys. Rev. Lett.* **199:** , *77*, 1632–1635.
[24] a) S. Wang, H. Chen, J. Liu, C. Chen, M Liu, *Adv. Funct. Mater.* **2020**, *30*N b) C. Ren, X. I eng, W. Hu, J. Li, X. Miao, S. Xiao, H. Liu, Q. Fan, P. Wang, T. He, *Chem. Commun. (Camb.)* **2019**, *55*, 5111–5114Nc) T. G. Allen, S. Menis, N. Munera, J. Zhang, S. I ai, T. Li, M Jia, W. Wang, S. Marlow, I. J. Hagan, E. W. Van Stryland, X. Zhan, J. W. Perry, S. R. Marder, *J. Phys. Chem. A.* **2020**, *12A*, 4367–4378Nd) S. Wang, J. Liu, C. C. Goh, L. G. Ng, M Liu, *Adv. Mater.* **2019**, *31*, e1904447.
[25] T. Schwich, M. P. Cifuentes, P. A. Gugger, M. Samoc, M. G. Humphrey, *Adv. Mater.* **2011**, *23*, 1433–1435.
[26] a) P.-H. Huang, J.-Y. Shen, S.-C. Pu, Y.-S. Wen, J. T. Lin, P.-T. Chou, M.-C. P. Yeh, *J. Mater. Chem.* **200:** , *16*, 850–857N b) J. P. Zareba, M. Nyk, M. Samoc, *Polymers* (Masel) **2020**, *12*.
[27] a) M. Yang, C. Mo, L. Fang, J. Li, Z. Yuan, Z. Chen, Q. Jiang, X. Chen, I. Yu, *Adv. Funct. Mater.* **2020**, *30*, 2000516Nb) S. Lu, L. Sui, J. Liu, S. Zhu, A. Chen, M. Jin, M Yang, *Adv. Mater.* **2018**, *29*, 1603443Nc) L. Poocza, M. Gottschaldt, E. Markweg, N. Hauptmann, G. Hildebrand, I. Pretzel, M. Hartlieb, C. Reichardt, J. PUbel, K. S. Schubert, O. Mollenhauer, M Iietzek, P. Liefeith, *Adv. Eng. Mater.* **2018**, *19*, 1600686Nd) X. Wang, P. Li, Q. I ing, C. Wu, W. Zhang, M Tang, *J. Am. Chem. Soc.* **2019**, *1A1*, 2061–2068.
[28] Y. Wang, Y. Jiang, J. Hua, H. Tian, S. Qian, *J. Appl. Phys.* **2011**, *110*, 033518.
[29] Q. Mellier, N. S. Makarov, P. A. Mouit, S. Rigaut, P. Pamada, P. Feneyrou, G. Merginc, O. Maury, J. W. Perry, C. Andraud, *Phys. Chem. Chem. Phys.* **2012**, *1A*, 15299–15307.
[30] A. Medi, L. J. W. Shimon, O. Gidron, *J. Am. Chem. Soc.* **2017**, *1A0*, 8086–8090.
[31] T. Ozdemir, J. L. Mla, F. Sozmen, L. T. Yildirim, E. K. Akkaya, *Org. Lett.* **201:** , *18*, 4821–4823.
[32] L. Cheng, W. He, H. Gong, C. Wang, Q. Chen, Z. Cheng, Z. Liu, *Adv. Funct. Mater.* **2013**, *23*, 5893–5902.
[33] a) P. Mrochard, V. Grolier-Mazza, R. Cabanel, *J. Opt. Soc. Am. B* **1998**, *1A*, 405–414Nb) I. I. Povsh, I. J. Hagan, E. W. V. Stryland, *Opt. EDpress* **1999**, *A*, 315–327Nc) X. Li, P. Hu, M Lyu, J. Zhang, Y. Wang, P. Wang, S. Xiao, Y. Gao, J. He, *J. Phys. Chem. C.* **201:** , *120*, 18243–18248.
[34] R. A. Ganeev, A. I. Ryasnyansky, N. Ishizawa, M. Maba, M. Suzuki, M. Turu, S. Sakakibara, H. Puroda, *Optics Commun.* **200**, *231*, 431–436.

Manuscript receivedLNovember 16, 2020
Revised manuscript receivedLI ecember 17, 2020
Accepted manuscript onlineLI ecember 22, 2020
Version of record onlineLJanuary 14, 2021